

Experimental demonstration of switching entangled photons based on the Rydberg blockade effect

Yi-Chen Yu,^{1,2} Ming-Xin Dong,^{1,2} Ying-Hao Ye,^{1,2} Guang-Can Guo,^{1,2} Dong-Sheng Ding,^{1,2,*} and Bao-Sen Shi^{1,2,†}

¹*Key Laboratory of Quantum Information, University of Science and Technology of China, Hefei, Anhui 230026, China.*

²*Synergetic Innovation Center of Quantum Information and Quantum Physics, University of Science and Technology of China, Hefei, Anhui 230026, China.*

(Dated: November 3, 2020)

The long-range interaction between Rydberg-excited atoms endows a medium with large optical nonlinearity. Here, we demonstrate an optical switch to operate on a single photon from an entangled photon pair under a Rydberg electromagnetically induced transparency configuration. With the presence of the Rydberg blockade effect, we switch on a gate field to make the atomic medium nontransparent thereby absorbing the single photon emitted from another atomic ensemble via the spontaneous four-wave mixing process. In contrast to the case without a gate field, more than 50% of the photons sent to the switch are blocked, and finally achieve an effective single-photon switch. There are on average 1~2 gate photons per effective blockade sphere in one gate pulse. This switching effect on a single entangled photon depends on the principal quantum number and the photon number of the gate field. Our experimental progress is significant in the quantum information process especially in controlling the interaction between Rydberg atoms and entangled photon pairs.

Keywords: Rydberg blockade, entangled photon, quantum switch

Pacs numbers: 32.80.Rm, 42.50.Gy, 42.50.Ct, 42.50.Nn

1. Introduction

In analogy to classical electronic counterparts, quantum switches are regarded as basic building blocks for quantum circuits and networks [1–4]. Switching states in the full-quantum regime where single particles control a quantum qubit or entanglement from another system may enable further applications in quantum information science, such as in quantum computing [5], distributed quantum information processing [6–8], and metrology [9]. Many efforts have been done towards constructing a prototype; examples include a micro-resonator coupled with a single atom [10], cold atoms trapped in a microscopic hollow fiber [11], cold atoms coupled to a cavity [12], strongly coupled quantum cavity-dots [13], and single dye molecules [14].

The strong interaction offered by Rydberg-excited atoms shifts the energy levels of the surrounding atoms dramatically and suppresses all further excitation of these neighboring atoms. This interaction between cold atoms gives rise to excitation blockade [15–21], multipartite entanglement [22–25], spatial correlations [26–28], strong optical nonlinearities [29–35], plasma formation [36], and photon-photon gate [37]. The single-photon nonlinearity arising from the strong interaction between Rydberg atoms shows great potential in constructing single-photon transistors [38–40]. The fundamental aspects of quantum nonlinearity based on Rydberg atoms have been studied before; a type of "photonic hourglass" single-photon device is constructed [31, 41]. Such "photonic

hourglass" is a kind of medium exhibiting strong absorption of photon pairs while remaining transparent to single photons. However, all the relative experiments on switching were demonstrated with a weak coherent field, thus there are no reports on switching of a true single-photon. Operating on true single photons is more challenging than attenuated coherent pulses.

Here, we demonstrate an experiment of switching true single-photons from entangle photon pairs. The entangled photon pairs are prepared in one atomic cloud and propagate through another atomic cloud for switching operation. The switching operation is using a single-photon level gate field to turn on or turn off the acceptance of that true single-photon. We prepare a gate pulse with 1~2 photons per blockade sphere to switch one of the entangled photons based on Rydberg blockade effect. By controlling the large nonlinearity offered by the long-range interaction from the Rydberg atoms, we can turn on and turn off the Rydberg electromagnetically induced transparency (Rydberg-EIT) window corresponding to the switch on and switch off operation [29, 42]. The measured coincidence counts with and without a gate field show an obvious switching effect of the entangled photons. The fidelity of the entangled state is $85.3\% \pm 1.5\%$ and $80.4\% \pm 2.3\%$ in the absence and presence of a gate field, respectively, with a switch contrast larger than 50%. By increasing the principal quantum number n , the switching effect becomes stronger and the required photon number of the gate field decreases. Implementing a Rydberg-mediated switch device under non-classical fields could enable the implementation of quantum computation and information processing with the interaction between Rydberg atoms and entangled photons [5], such as building a Toffoli gate [43] and quantum computation [44–47] with Rydberg ensembles, and switching a distributed quantum node.

2. Results

2.1. Experimental setup

The sample media are optically thick atomic ensembles of Rubidium 85 (^{85}Rb) trapped in different magneto-optic traps (MOTs), labeled MOT 1 and MOT 2. Schematics of the energy levels, time sequence, and experimental setup are shown in figure 1 (a)–(c). A cigar-shaped ^{85}Rb atomic ensemble is first prepared in MOT 1 and then cooled down to about 100 μK via the optical molasses technique; the atomic cloud has dimensions of $10 \times 2 \times 2 \text{ mm}^3$. We prepare non-classical photon pairs by spontaneous four-wave mixing (SFWM) in this atomic ensemble. The energy levels involved here correspond to the double- Λ system, consisting of both the D1 and D2 lines of Rubidium 85. The two pump fields couple the atomic transition $5S_{1/2}(F=3) \rightarrow 5P_{1/2}(F'=3)$ with a detuning of $-2\pi \times 110 \text{ MHz}$ and the atomic transition $5S_{1/2}(F=2) \rightarrow 5P_{3/2}(F'=3)$ under resonance. The generated signal photons (labeled signal 1 and signal 2) are correlated in the time domain. The signal-2 photon passing through an acousto-optic modulator (AOM) is frequency shifted by $+2\pi \times 120 \text{ MHz}$, after which it is exactly resonant with the atomic transition $5S_{1/2}(F=3) \rightarrow 5P_{3/2}(F'=4)$. Then, the signal-2 photon propagates through the three-dimensional ^{85}Rb atomic cloud in MOT 2 for the demonstration of the switching process. Finally, we perform quantum state tomography for the photonic entanglement before two signals are detected by two single-photon detectors. The coils of MOT 2 are switched off during the switching measurement. The spherical atomic cloud of MOT 2 has a size of 500 μm with a temperature $\sim 20 \mu\text{K}$ and an average density of $3.5 \times 10^{11} \text{ cm}^{-3}$. The coupling field is resonant with the atomic transition $5P_{3/2}(F'=4) \rightarrow |nD_{5/2}\rangle$, that is $\Delta_c = 0$. Rabi frequency of coupling light is $\Omega_c = 2\pi \times 11 \text{ MHz}$ to demonstrate EIT and blockade configuration for single-photons.

The signal-2 photon has a beam waist of 16 μm in the center of MOT 2 which is obtained by using a short-focus lens. With a pulsed coupling beam (TA-SHG, Toptica), we demonstrate Rydberg-EIT in the ladder-type atomic configuration, consisting of a ground state $|g\rangle$, an excited state $|e\rangle$, and a highly-excited state $|nD\rangle$; here, $n = 50$. The gate field has a beam waist of 18 μm in the center of MOT 2 and couples the atomic transition $5S_{1/2}(F=3) \rightarrow 5P_{3/2}(F'=4)$. The coupling field with a beam waist of 30 μm covers both the gate and signal-2 beams. The smaller the beam waist, the stronger the blockade effect [31]. However the beam size is limited to the size of the transmission window of our MOT. Analyzing the van der Waals interactions between the Rydberg atoms with an effective coefficient $\bar{C}_6 = 2\pi \times 32 \text{ GHz} \cdot \mu\text{m}^6$

for the rubidium $50D_{5/2}$ by considering weighted average of the interaction effects of all Zeeman sublevels, we can calculate an average blockade radius $\sim 3.78 \mu\text{m}$ with $\bar{r}_b = \left| \frac{\bar{C}_6}{\sqrt{(2\Delta_c)^2 + \Omega_c^2}} \right|^{1/6}$ [48] [49]. Since the coupling Rabi frequency is larger than the bandwidth of the signal photon, we use the strong coupling configuration to calculate the blockade radius. Figure 1(d) describes the switching effect on a weak coherent pulse, the red and blue lines represent the Rydberg-EIT spectra with and without a coherent gate field.

2.2. Bandwidth matching

In order to switch single photons, we need to connect two physical systems. One is to generate entangled photon; the other is to operate on that photon. We match the frequency and the bandwidth between the signal-2 photon and the absorption window of the atomic ensemble in MOT 2. This can be realized by changing the frequency and Rabi frequency Ω_{p2} of the pump 2 field as explained above. The switching effect obviously decreases when the bandwidth of signal-2 photon increases. Due to the narrow transparency window in the spectrum of Rydberg-EIT, the optical response on two-photon resonance is strongly affected by the level shifts induced by Rydberg atoms interaction and the linewidths of the input lasers [50]. Compared with S state, D state has wider transparency window resulting from the larger dipole matrix element to D state. Thus, we use Rydberg- D state to get larger bandwidth and higher transmission rate of Rydberg-EIT window.

As a result, the mismatching between the signal-2 photon and the absorption bandwidth of the atomic ensemble in MOT 2 decreases the switch contrast. Because the high-frequency component of the signal-2 photon is unable to fall within the Rydberg-EIT window, the reabsorption of the signal-2 photon weakens although the gate field is present. The switch contrast decreases with increasing Rabi frequency Ω_{p2} of pump 2 field (see figure 2). The bandwidth of the signal-2 photon depends significantly on Ω_{p2} [51, 52], because the profile of the wave packet of the signal-2 photon can be modulated by tuning the Λ -EIT transparency window. The single-photon bandwidth becomes narrower with the Ω_{p2} decreasing. Only when the bandwidth of the single photon is narrower than the Rydberg-EIT window, can we get a higher absorption rate and switch contrast. This data in figure 2 hints that the switching effect becomes more obvious with a smaller Ω_{p2} . For the optimized case $\Omega_{p2} \sim 2\pi \times 1 \text{ MHz}$, the bandwidth of the signal-2 photon is at $\sim 2\pi \times 5 \text{ MHz}$, and the absorption window for the atomic ensemble in MOT 2 is $\sim 2\pi \times 13 \text{ MHz}$. That is, the signal-2 photon can completely fall within the Rydberg-EIT window. If decreasing Ω_{p2} further, the signal to noise ratio of two-photon coincidence becomes worse.

2.3. Switch entangled photons

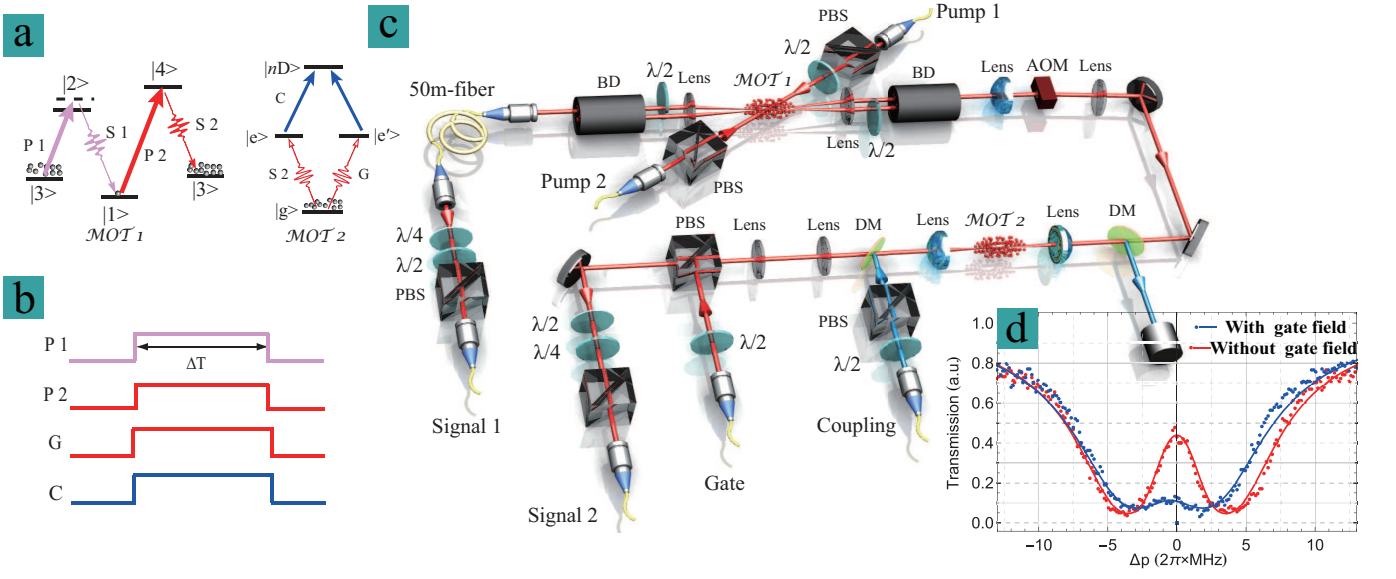


Figure 1. (a) Energy diagram of entanglement generation and the switching processes. The double- Λ atomic configuration corresponds to the ^{85}Rb states $5S_{1/2}(F=2)$ ($|1\rangle$), $5P_{1/2}(F'=3)$ ($|2\rangle$), $5S_{1/2}(F=3)$ ($|3\rangle$), and $5P_{3/2}(F'=3)$ ($|4\rangle$), respectively. The pump fields are P1 and P2 and the signal fields are S1 and S2. The right-side energy diagram is a ladder-type energy level with ground state $5S_{1/2}(F=3)$ ($|g\rangle$), excited state $5P_{3/2}(F'=4)$ ($|e\rangle$), and highly-excited state $|nD_{5/2}\rangle$ ($|nD\rangle$). Labels: P-pump, S-signal. (b) Time sequence for the preparation and switching on single photons. ΔT represents the experimental time window. (c) Schematic overview of the experimental setup. Labels: PBS-polarizing beam splitter, DM-dichroic mirror, AOM-acousto-optic modulator. (d) The Rydberg-EIT transmission spectra is recorded with and without the gate field when $n = 50$. The solid lines are fitted by the function $e^{-2\text{Im}[w_{s2}/c(1+\chi/2)]L}$ with $OD = 8$, $\Omega_c = 2\pi \times 6.8$ MHz, $\delta\Delta = 2\pi \times 0$ MHz, $\gamma_{rg} = 2\pi \times 0.03$ MHz, $\Gamma_{de} = 2\pi \times 0.07$ MHz and $OD = 8$, $\Omega_c = 2\pi \times 5$ MHz, $\delta\Delta = 2\pi \times 0.5$ MHz, $\gamma_{rg} = 2\pi \times 2.5$ MHz for red and blue data, respectively. The fitted function and these parameters are defined in theoretical analysis part in supplementary materials.

To demonstrate the switching effect under quantum regime, we firstly prepared non-classical photon pairs via SFWM process [51, 52] in MOT 1. The generated photon pairs are correlated in time domain. We construct two optical paths L and R by using two beam displacers (BDs) to build a passive-locking interferometer [53–55] where the perturbations between L and R optical paths can be mutually eliminated. The signal photons in each path are collinear, as the phase matching con-

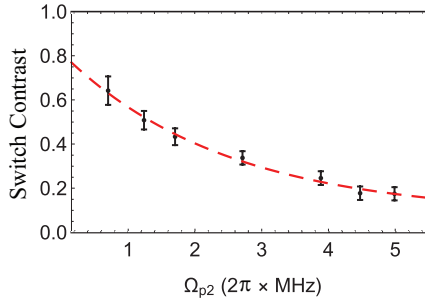


Figure 2. The measured switch contrast against with Ω_{p2} , the solid red curve is guided for eye which is fitted by a function $y = A * \text{Exp}[-x/t] + y_0$ with parameters of $A = 0.73481$; $y_0 = 0.07865$; $t = 2.45$.

dition $k_{p1} - k_{s1} = k_{p2} - k_{s2}$ should be satisfied in the SFWM process. With two half-wave plates inserted in the R optical path, the signal photons along these two optical paths can be coherently combined by BDs. The form of the entanglement is

$$|\psi\rangle = (|H_{s1}\rangle |V_{s2}\rangle + e^{i\theta} |V_{s1}\rangle |H_{s2}\rangle) / \sqrt{2} \quad (1)$$

with θ , the relative phase between L and R optical paths, setting to zero in our experiment; $|H_{s1,s2}\rangle$ and $|V_{s1,s2}\rangle$ represent the horizontal and vertical polarized states of the signal photons. The details about generating entan-

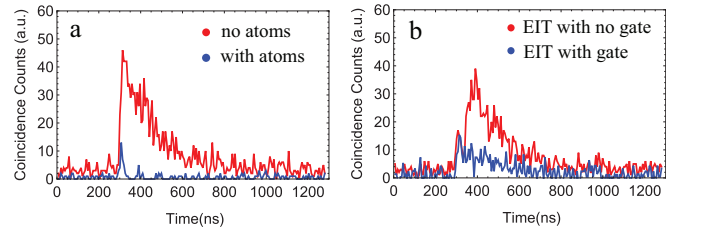


Figure 3. Coincidence counts (CC) under different situations corresponding to: (a) with (blue) and without atoms (red), and (b) under the Rydberg-EIT configuration with (blue) and without (red) gate field. All of these CC were detected in 4000 s.

gled photon pair are in our supplementary materials.

In order to demonstrate the switching effect of entangled photons, we input entangled photons into MOT 2. In this situation, we use a 50-m fibre to introduce a time delay in the path of the signal-1 photons. This guarantees that the entanglement does not collapse before the switching process has finished. The results are shown in figure 3(a) and (b); the former shows the coincidence counts of photon pairs when the atoms in MOT 2 are absent (red) and present (blue), whereas the latter shows the results under Rydberg-EIT without (red) and with (blue) gate field. Obviously, the coincidence counts decrease when the gate field is applied as the signal-2 photon is significantly absorbed when compared with the no-gate situation. The central physics behind the operation of a single-photon switch is that the long-range interaction between Rydberg atoms endows the Rydberg-EIT medium with a large optical nonlinearity [31, 56], and the resulting dipole blockade effect makes the medium non-transparent. We define a switch contrast to characterize the switching effect,

$$C_{\text{switch}} = \frac{CC_{\text{EIT}} - CC_{\text{gate}}}{CC_{\text{EIT}}}, \quad (2)$$

where CC_{EIT} and CC_{gate} represent the total coincidence counts between the signal-1 and signal-2 photons without and with a gate field. From the data [figure 3 (a) and (b)], we obtain a switch contrast of $C_{\text{switch}} = 77.6\% \pm 3.1\%$. The little peak in the rising edge comes from the high-frequency components of the single photons, which falls out of the absorption window of the atoms, [marked in blue color in figure 3 (a)]. In our experiment, the absorption window of atoms in MOT 2 is about $\sim 2\pi \times 13$ MHz. Although the bandwidth of the signal-2 photon wavepacket may be tuned by decreasing the power of pump 2 field [52], there is always a high-frequency component in the wavepacket of the signal-2 photon. And the component falls outside of the bandwidth of the absorption, which induces an optical precursor [57, 58]. The switch contrast is also limited by the broadening effect of the Rydberg-EIT window, which is maybe caused by the dephasing of the distribution of Rabi frequencies with the unpolarized atoms in MOT 2. Our experiment is demonstrated with no bias magnetic fields. The atoms can be treated as averagely distributed in all sublevels.

We change the detected state φ_{s2} of the signal-2 photon and recorded the coincidence counts under different signal-1 states φ_{s1} of $|H\rangle$, $|V\rangle$, $|H\rangle - i|V\rangle$, and $|H\rangle + |V\rangle$. To obtain the differences with and without the gate field, we recorded these coincidence counts under these situations [figure 4 (a)–(d)]. The coincidence counts without (semi-transparent blue)/with (blue) the gate field are obviously different. We obtain switch contrasts with $C_{\text{switch}}^{VH} = 81.0\%$, $C_{\text{switch}}^{HV} = 64.3\%$, $C_{\text{switch}}^{RR} = 52.2\%$, and

$C_{\text{switch}}^{DD} = 79.9\%$ under the four situations $\varphi_{s1} = |V\rangle$, $\varphi_{s2} = |H\rangle$; $\varphi_{s1} = |V\rangle$, $\varphi_{s2} = |H\rangle$; $\varphi_{s1} = \varphi_{s2} = |H\rangle - i|V\rangle$ and $\varphi_{s1} = \varphi_{s2} = |H\rangle + |V\rangle$. The switching operation is effective for any polarization state with treating the signal-2 photon as if it were in a mixed state. The obtained switching contrasts are different depending on the detected states due to the non-perfect balance of the photon generation rate in the two optical paths and the noise of each path. In addition, we measure two-photon interference without and with the gate field under the signal-2 basis of $|H\rangle$ and $|H\rangle + |V\rangle$ [figure 4 (e) and (f)]. From figure 4 (e), we find the visibility without the gate field exceeding the threshold 70.7%, which means that the entanglement can be preserved after the transmission through the EIT window. It is easy to observe that the propagation of the signal-2 photon through the Rydberg-EIT medium doesn't destroy the entanglement, because the Rydberg-EIT is independent on the polarization of the signal-2 photon.

We also perform quantum state tomography [59] for the photonic entanglement to compare the entanglement properties before and after the switching process. Signal-1 and signal-2 are polarization entangled, their entangled state being $|\psi\rangle = (|H\rangle_{s1}|V\rangle_{s2} + |V\rangle_{s1}|H\rangle_{s2})/\sqrt{2}$. Using the polarizing beam splitter, half-wave plate, and quarter-wave plate, we project the two photon states onto the four polarization states $|\phi_{1\sim 4}\rangle$ ($|H\rangle$, $|V\rangle$, $(|H\rangle - i|V\rangle)/\sqrt{2}$, $(|H\rangle + |V\rangle)/\sqrt{2}$). We obtain a set of 16 data points from which to reconstruct the density matrix. By comparing with the ideal density matrix ρ_{ideal} using the formula $F_i = \text{Tr}(\sqrt{\sqrt{\rho}\rho_{\text{ideal}}\sqrt{\rho}})^2$, we obtain the fidelity to be $87.1\% \pm 2.5\%$ corresponding to the fidelity of input photons. By comparing with the input density matrix using the formula of $F = \text{Tr}(\sqrt{\sqrt{\rho_{\text{output}}}\rho_{\text{input}}\sqrt{\rho_{\text{output}}}})^2$, the fidelity for the output state without gate field is $85.3\% \pm 1.5\%$, and the state with gate field is $80.4\% \pm 2.3\%$. The switch contrast does not dramatically decrease before and after switch process. We use the initial fidelity for the input state to characterize the entanglement of the entangled photon pairs from SFWM process. Then, we want to demonstrate that our switching operation is a quantum process without any destructive effect to the input entanglement by calculating the fidelity for the output state with and without the gate field, respectively. We can still get high fidelity of the entanglement via much longer detecting time after the transmission through the EIT window, as if we hadn't operated on it.

The nonlinearity of the medium not only depends on the atomic density, which determines the interaction distance, but also is strongly affected by the dipole interaction strength. We change the principal quantum number n to change the interaction strength to measure both the Rydberg-EIT transmission contrast and the switch contrast. Here the Rydberg-EIT contrast is defined as $C_{\text{EIT}} = (CC_{\text{no-atom}} - CC_{\text{EIT}})/CC_{\text{no-atom}}$,

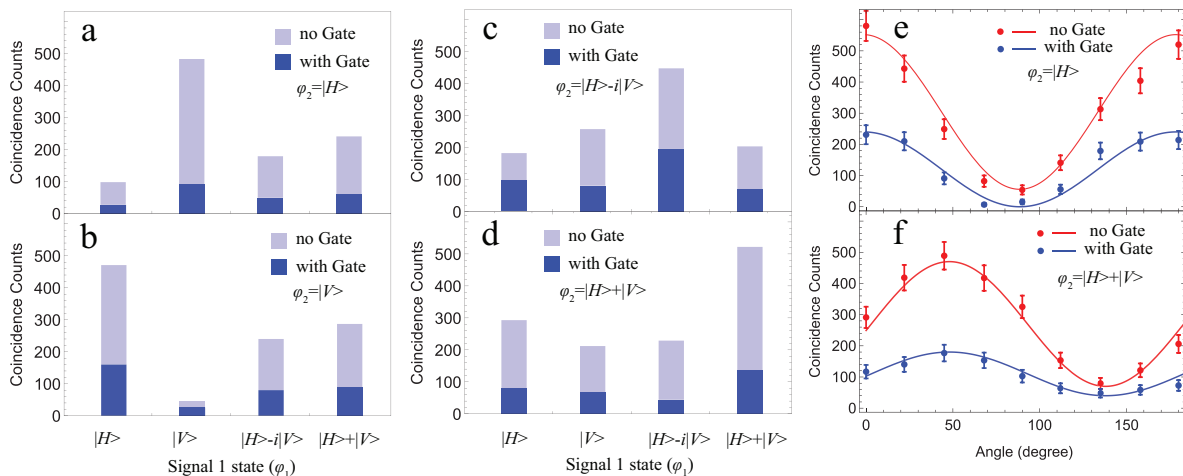


Figure 4. Switching with different bases: (a)–(d) are the coincidence counts without a gate field (semi-transparent blue column) and with a gate field (blue column) under different signal-1 states of $|H\rangle$, $|V\rangle$, $|H\rangle - i|V\rangle$, and $|H\rangle + |V\rangle$. (e) and (f) are the recorded two-photon interference curves with signal-2 states of $|H\rangle$ and $|H\rangle + |V\rangle$ without gate field (red) and with gate field (blue). Their interference visibilities are $87.0\% \pm 0.8\%$ ((e), red), $82.9\% \pm 0.7\%$ ((e), blue), $72.0\% \pm 1.1\%$ ((f), red), and $57.1\% \pm 2.6\%$ ((f), blue). The solid lines are fitted curves to the measured data. All these coincidence counts were recorded over a interval of 1000 s. Error bars are ± 1 standard deviation.

$CC_{\text{no_atom}}$ representing the total coincidence counts between the signal-1 and signal-2 photons without atoms. We change the principal quantum number n by changing the wavelength of the coupling laser. Each time we change the wavelength, we adjust the experimental optical system to keep the coupling Rabi frequency a constant. The results (figure 5) show that the Rydberg-EIT contrast decreases with the increase of n ; this is because the transition amplitude for $|e\rangle \rightarrow |nD\rangle$ decreases. In contrast, because the dipole interaction strength increases, the switch contrast of the signal-2 photon obviously increases by comparing two situations, $n = 60$ ($\bar{r}_b = 5.12 \mu\text{m}$) and $n = 40$ ($\bar{r}_b = 1.05 \mu\text{m}$). The switch contrast is larger than 50% when $n > 45$, revealing an effective switching operation. In this way, the interaction between Rydberg atoms becomes stronger with the principal quantum number increasing. Although the gate field has hundreds of photons because of the relatively large size of the atomic cloud in our experiment, we calculate that there are on average $1 \sim 2$ gate photons per effective blockade sphere corresponding to the average energy of the gate field inside a blockade sphere expressed in units of $\hbar * \omega$. Eventually, the single-photon switch with a single gate photon can be realized by trapping the atoms into the scale of the blockade radius and increasing the principal quantum number n .

3. Discussion

In addition, in order to avoid saturation of our switch system where the gate and coupling field would deplete the atoms after a certain duration, we set the experimental time window to $25 \mu\text{s}$. The lifetime of Rydberg-excited atom is estimated to be ~ 800 ns by measuring

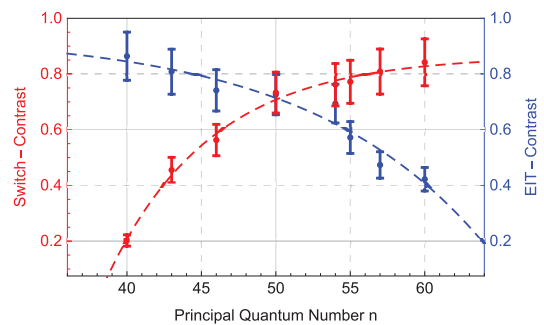


Figure 5. Dependence of the switch contrast (red) and Rydberg-EIT contrast (blue) on the principal quantum number. As visual guides, the data are fitted with function $y = A * \text{Exp}[-x/t] + y_0$ (dotted lines) with parameter settings $A = -0.00327$, $y_0 = 0.94$, $t = -11.77$ and $A = -198.23$, $y_0 = 0.87$, $t = 7.0$. In this process, the gate field intensity is set to average ~ 2 gate photons per effective blockade sphere. Error bars are ± 1 standard deviation.

the Rydberg spinwave through storage process [53, 60], which guarantees an adequate interaction time for each switch operation during near 200 ns arrival time of the signal-2 photon given in figure 3. In our experiment, the dephasing of Rydberg D state [33] is not obvious due to the small gate photon numbers used here. With small photon numbers as input, we have not investigated an obvious time dependence of the transmission on Rydberg-EIT resonance, but with an obvious time dependence of the transmission for large photon numbers, more details are shown in supplementary materials figure 2. Thus, the nonlinearity behind the switch experiment is offered by Rydberg blockade effect (see

more details in supplementary materials figure 3). Besides, there are some challenges to improve the switch contrast: 1. Decreasing the bandwidth mismatch between signal-photon and the Rydberg-EIT transparency window. 2. Increasing the principle quantum number n to achieve large dipole-dipole interaction strength, as shown in figure 5. 3. Trapping the atoms into the scale of the blockade radius. 4. Using a single-photon with ultra-narrow bandwidth. The bandwidth of transparency window of Rydberg-EIT with large principle quantum number n would become narrower due to smaller natural line width for high- n Rydberg state. This means that it needs narrower bandwidth of single-photon, such as subnatural-linewidth single-photon source [52].

In summary, we have demonstrated an optical switch on entangled photons based on Rydberg nonlinearity with two atomic ensembles. The emitted signal-2 photon correlated with the signal-1 photon is blocked by another gate field under the Rydberg-EIT configuration. Switching effect depends on the principal quantum number, the bandwidth of the emitted single photons, and the average photon number of the gate field. We have successfully realized optical switch on one of the entangled photons of the pair, with more than 50% of pairs being blocked. These results on switching single photons using the strong dipole interaction hold promises in demonstrating quantum information processing between Rydberg atoms and entangled photons.

4. Acknowledgements

The authors thank Prof. Lin Li from huazhong university of science and technology and Prof. Yuan Sun from national university of defense technology for valued discussions and critical reading our manuscript. This work was supported by National Key Research and Development Program of China (2017YFA0304800), the National Natural Science Foundation of China (Grant Nos. 61525504, 61722510, 61435011, 11174271, 61275115, 11604322), Anhui Initiative in Quantum Information Technologies (AHY020200), and the Youth Innovation Pro motion Association of Chinese Academy of Sciences under Grant No. 2018490.

* dds@ustc.edu.cn

† drshi@ustc.edu.cn

- [1] Juan Ignacio Cirac, Peter Zoller, H Jeff Kimble, and Hideo Mabuchi, “Quantum state transfer and entanglement distribution among distant nodes in a quantum network,” *Phys. Rev. Lett.* **78**, 3221 (1997).
- [2] Jeremy L O’Brien, Akira Furusawa, and Jelena Vučković, “Photonic quantum technologies,” *Nat. Photon.* **3**, 687 (2009).
- [3] H John Caulfield and Shlomi Dolev, “Why future super-computing requires optics,” *Nat. Photon.* **4**, 261 (2010).
- [4] Feng Wang, Ming-Xing Luo, Gang Xu, Xiu-Bo Chen, and Yi-Xian Yang, “Photonic quantum network transmission assisted by the weak cross-kerr nonlinearity,” *Science China Physics, Mechanics & Astronomy* **61** (2018), 10.1007/s11433-017-9143-y.
- [5] Mark Saffman, TG Walker, and Klaus Mølmer, “Quantum information with rydberg atoms,” *Reviews of Modern Physics* **82**, 2313 (2010).
- [6] H Jeff Kimble, “The quantum internet,” *Nature* **453**, 1023 (2008).
- [7] Zheng-Xia Cui, Wei Zhong, Lan Zhou, and Yu-Bo Sheng, “Measurement-device-independent quantum key distribution with hyper-encoding,” *Science China Physics, Mechanics & Astronomy* **62** (2019), 10.1007/s11433-019-1438-6.
- [8] XinCheng Xie, “Quantum secure direct communication with an untrusted charlie using imperfect measurement devices,” *Science China Physics, Mechanics & Astronomy* **63** (2020), 10.1007/s11433-019-1491-1.
- [9] Peter Komar, Eric M Kessler, Michael Bishof, Liang Jiang, Anders S Sørensen, Jun Ye, and Mikhail D Lukin, “A quantum network of clocks,” *Nat. Phys.* **10**, 582 (2014).
- [10] Danny O’Shea, Christian Junge, Jürgen Volz, and Arno Rauschenbeutel, “Fiber-optical switch controlled by a single atom,” *Phys. Rev. Lett.* **111**, 193601 (2013).
- [11] Michal Bajcsy, Sebastian Hofferberth, Vlatko Balic, Thibault Peyronel, Mohammad Hafezi, Alexander S Zibrov, Vladan Vuletic, and Mikhail D Lukin, “Efficient all-optical switching using slow light within a hollow fiber,” *Phys. Rev. Lett.* **102**, 203902 (2009).
- [12] Wenlan Chen, Kristin M Beck, Robert Bücker, Michael Gullans, Mikhail D Lukin, Haruka Tanji-Suzuki, and Vladan Vuletić, “All-optical switch and transistor gated by one stored photon,” *Science*, 1237242 (2013).
- [13] Thomas Volz, Andreas Reinhard, Martin Winger, Antonio Badolato, Kevin J Hennessy, Evelyn L Hu, and Ataç Imamoglu, “Ultrafast all-optical switching by single photons,” *Nat. Photon.* **6**, 605 (2012).
- [14] Jaesuk Hwang, Martin Pototschnig, Robert Lettow, Gert Zumofen, Alois Renn, Stephan Götzinger, and Vahid Sandoghdar, “A single-molecule optical transistor,” *Nature* **460**, 76 (2009).
- [15] Daniel Comparat and Pierre Pillet, “Dipole blockade in a cold rydberg atomic sample [invited],” *JOSA B* **27**, A208–A232 (2010).
- [16] D Jaksch, JI Cirac, P Zoller, SL Rolston, R Côté, and MD Lukin, “Fast quantum gates for neutral atoms,” *Phys. Rev. Lett.* **85**, 2208 (2000).
- [17] MD Lukin, M Fleischhauer, R Cote, LM Duan, D Jaksch, JI Cirac, and P Zoller, “Dipole blockade and quantum information processing in mesoscopic atomic ensembles,” *Phys. Rev. Lett.* **87**, 037901 (2001).
- [18] D Tong, SM Farooqi, J Stanojevic, S Krishnan, YP Zhang, R Côté, EE Eyler, and PL Gould, “Local blockade of rydberg excitation in an ultracold gas,” *Phys. Rev. Lett.* **93**, 063001 (2004).
- [19] Kilian Singer, Markus Reetz-Lamour, Thomas Amthor, Luis Gustavo Marcassa, and Matthias Weidemüller, “Suppression of excitation and spectral broadening induced by interactions in a cold gas of rydberg atoms,” *Phys. Rev. Lett.* **93**, 163001 (2004).
- [20] E Urban, Todd A Johnson, T Henage, L Isenhower, DD Yavuz, TG Walker, and M Saffman, “Observation

- of rydberg blockade between two atoms,” *Nature Physics* **5**, 110 (2009).
- [21] Alpha Gaëtan, Yevhen Miroshnychenko, Tatjana Wilk, Amodsen Chotia, Matthieu Viteau, Daniel Comparat, Pierre Pillet, Antoine Browaeys, and Philippe Grangier, “Observation of collective excitation of two individual atoms in the rydberg blockade regime,” *Nat. Phys.* **5**, 115 (2009).
- [22] Rolf Heidemann, Ulrich Raitzsch, Vera Bendkowsky, Björn Butscher, Robert Löw, Luis Santos, and Tilman Pfau, “Evidence for coherent collective rydberg excitation in the strong blockade regime,” *Phys. Rev. Lett.* **99**, 163601 (2007).
- [23] Johannes Zeiher, Peter Schauß, Sebastian Hild, Tommaso Macrì, Immanuel Bloch, and Christian Gross, “Microscopic characterization of scalable coherent rydberg superatoms,” *Phys. Rev. X* **5**, 031015 (2015).
- [24] Henning Labuhn, Daniel Barredo, Sylvain Ravets, Sylvain De Léséleuc, Tommaso Macrì, Thierry Lahaye, and Antoine Browaeys, “Tunable two-dimensional arrays of single rydberg atoms for realizing quantum ising models,” *Nature* **534**, 667–684 (2016).
- [25] Hannes Bernien, Sylvain Schwartz, Alexander Keesling, Harry Levine, Ahmed Omran, Hannes Pichler, Soonwon Choi, Alexander S Zibrov, Manuel Endres, Markus Greiner, *et al.*, “Probing many-body dynamics on a 51-atom quantum simulator,” *Nature* **551**, 579 (2017).
- [26] Peter Schauß, Marc Cheneau, Manuel Endres, Takeshi Fukuhara, Sebastian Hild, Ahmed Omran, Thomas Pohl, Christian Gross, Stefan Kuhr, and Immanuel Bloch, “Observation of spatially ordered structures in a two-dimensional rydberg gas,” *Nature* **491**, 87–91 (2012).
- [27] Andrew Schwarzkopf, RE Sapiro, and Georg Raithel, “Imaging spatial correlations of rydberg excitations in cold atom clouds,” *Phys. Rev. Lett.* **107**, 103001 (2011).
- [28] Peter Schauß, Johannes Zeiher, Takeshi Fukuhara, Sebastian Hild, Marc Cheneau, T Macrì, Thomas Pohl, Immanuel Bloch, and Christian Groß, “Crystallization in ising quantum magnets,” *Science* **347**, 1455–1458 (2015).
- [29] Jonathan D Pritchard, D Maxwell, Alexandre Gauguier, Kevin J Weatherill, MPA Jones, and Charles S Adams, “Cooperative atom-light interaction in a blocked rydberg ensemble,” *Phys. Rev. Lett.* **105**, 193603 (2010).
- [30] YO Dudin and A Kuzmich, “Strongly interacting rydberg excitations of a cold atomic gas,” *Science* **336**, 887–889 (2012).
- [31] Thibault Peyronel, Ofer Firstenberg, Qi-Yu Liang, Sebastian Hofferberth, Alexey V Gorshkov, Thomas Pohl, Mikhail D Lukin, and Vladan Vuletić, “Quantum nonlinear optics with single photons enabled by strongly interacting atoms,” *Nature* **488**, 57–60 (2012).
- [32] D Maxwell, DJ Szwed, D Paredes-Barato, H Busche, JD Pritchard, Alexandre Gauguier, KJ Weatherill, MPA Jones, and CS Adams, “Storage and control of optical photons using rydberg polaritons,” *Phys. Rev. Lett.* **110**, 103001 (2013).
- [33] Christoph Tresp, Przemyslaw Bienias, Sebastian Weber, Hannes Gorniaczyk, Ivan Mirgorodskiy, Hans Peter Büchler, and Sebastian Hofferberth, “Dipolar dephasing of rydberg d-state polaritons,” *Phys. Rev. Lett.* **115**, 083602 (2015).
- [34] Ofer Firstenberg, Charles S Adams, and Sebastian Hofferberth, “Nonlinear quantum optics mediated by rydberg interactions,” *Journal of Physics B: Atomic, Molecular and Optical Physics* **49**, 152003 (2016).
- [35] Callum R Murray and Thomas Pohl, “Coherent photon manipulation in interacting atomic ensembles,” *Phys. Rev. X* **7**, 031007 (2017).
- [36] M Robert-de Saint-Vincent, CS Hofmann, H Schempp, G Günter, S Whitlock, and M Weidemüller, “Spontaneous avalanche ionization of a strongly blocked rydberg gas,” *Phys. Rev. Lett.* **110**, 045004 (2013).
- [37] Daniel Tiarks, Steffen Schmidt-Eberle, Thomas Stolz, Gerhard Rempe, and Stephan Dürr, “A photon-photon quantum gate based on rydberg interactions,” *Nature Physics* **15**, 124 (2019).
- [38] Daniel Tiarks, Simon Baur, Katharina Schneider, Stephan Dürr, and Gerhard Rempe, “Single-photon transistor using a förster resonance,” *Phys. Rev. Lett.* **113**, 053602 (2014).
- [39] Hannes Gorniaczyk, Christoph Tresp, Johannes Schmidt, Helmut Fedder, and Sebastian Hofferberth, “Single-photon transistor mediated by interstate rydberg interactions,” *Phys. Rev. Lett.* **113**, 053601 (2014).
- [40] Simon Baur, Daniel Tiarks, Gerhard Rempe, and Stephan Dürr, “Single-photon switch based on rydberg blockade,” *Phys. Rev. Lett.* **112**, 073901 (2014).
- [41] Ofer Firstenberg, Thibault Peyronel, Qi-Yu Liang, Alexey V Gorshkov, Mikhail D Lukin, and Vladan Vuletić, “Attractive photons in a quantum nonlinear medium,” *Nature* **502**, 71–75 (2013).
- [42] David Petrosyan, Johannes Otterbach, and Michael Fleischhauer, “Electromagnetically induced transparency with rydberg atoms,” *Phys. Rev. Lett.* **107**, 213601 (2011).
- [43] David G Cory, MD Price, W Maas, E Knill, Raymond Laflamme, Wojciech H Zurek, Timothy F Havel, and SS Somaroo, “Experimental quantum error correction,” *Phys. Rev. Lett.* **81**, 2152 (1998).
- [44] Alexey V Gorshkov, Johannes Otterbach, Michael Fleischhauer, Thomas Pohl, and Mikhail D Lukin, “Photon-photon interactions via rydberg blockade,” *Physical review letters* **107**, 133602 (2011).
- [45] Mohammadsadegh Khazali, Khabat Heshami, and Christoph Simon, “Photon-photon gate via the interaction between two collective rydberg excitations,” *Physical Review A* **91**, 030301 (2015).
- [46] Andrew CJ Wade, Marco Mattioli, and Klaus Mølmer, “Single-atom single-photon coupling facilitated by atomic-ensemble dark-state mechanisms,” *Physical Review A* **94**, 053830 (2016).
- [47] Yuan Sun and Ping-Xing Chen, “Analysis of atom-photon quantum interface with intracavity rydberg-blocked atomic ensemble via two-photon transition,” *Optica* **5**, 1492–1501 (2018).
- [48] Jonathan B Balewski, Alexander T Krupp, Anita Gaj, Sebastian Hofferberth, Robert Löw, and Tilman Pfau, “Rydberg dressing: understanding of collective many-body effects and implications for experiments,” *New Journal of Physics* **16**, 063012 (2014).
- [49] Nikola Šibalić, Jonathan D Pritchard, Charles S Adams, and Kevin J Weatherill, “Arc: An open-source library for calculating properties of alkali rydberg atoms,” *Computer Physics Communications* **220**, 319–331 (2017).
- [50] Harry Levine, Alexander Keesling, Ahmed Omran, Hannes Bernien, Sylvain Schwartz, Alexander S Zibrov, Manuel Endres, Markus Greiner, Vladan Vuletić, and Mikhail D Lukin, “High-fidelity control and entangle-

- ment of rydberg-atom qubits,” *Physical review letters* **121**, 123603 (2018).
- [51] Shengwang Du, Jianming Wen, and Morton H Rubin, “Narrowband biphoton generation near atomic resonance,” *JOSA B* **25**, C98–C108 (2008).
- [52] Kaiyu Liao, Hui Yan, Junyu He, Shengwang Du, Zhi-Ming Zhang, and Shi-Liang Zhu, “Subnatural-linewidth polarization-entangled photon pairs with controllable temporal length,” *Phys. Rev. Lett.* **112**, 243602 (2014).
- [53] Dong-Sheng Ding, Kai Wang, Wei Zhang, Shuai Shi, Ming-Xin Dong, Yi-Chen Yu, Zhi-Yuan Zhou, Bao-Sen Shi, and Guang-Can Guo, “Entanglement between low- and high-lying atomic spin waves,” *Phys. Rev. A* **94**, 052326 (2016).
- [54] Wei Zhang, Dong-Sheng Ding, Ming-Xin Dong, Shuai Shi, Kai Wang, Shi-Long Liu, Yan Li, Zhi-Yuan Zhou, Bao-Sen Shi, and Guang-Can Guo, “Experimental realization of entanglement in multiple degrees of freedom between two quantum memories,” *Nat. Commun.* **7**, 13514 (2016).
- [55] Yi-Chen Yu, Dong-Sheng Ding, Ming-Xin Dong, Shuai Shi, Wei Zhang, and Bao-Sen Shi, “Self-stabilized narrow-bandwidth and high-fidelity entangled photons generated from cold atoms,” *Phys. Rev. A* **97**, 043809 (2018).
- [56] JD Pritchard, D Maxwell, Alexandre Gauguier, KJ Weatherill, MPA Jones, and CS Adams, “Cooperative atom-light interaction in a blockaded rydberg ensemble,” *Phys. Rev. Lett.* **105**, 193603 (2010).
- [57] Shanchao Zhang, JF Chen, Chang Liu, MMT Loy, George KL Wong, and Shengwang Du, “Optical precursor of a single photon,” *Phys. Rev. Lett.* **106**, 243602 (2011).
- [58] Dong-Sheng Ding, Yun Kun Jiang, Wei Zhang, Zhi-Yuan Zhou, Bao-Sen Shi, and Guang-Can Guo, “Optical precursor with four-wave mixing and storage based on a cold-atom ensemble,” *Physical review letters* **114**, 093601 (2015).
- [59] Daniel FV James, Paul G Kwiat, William J Munro, and Andrew G White, “Measurement of qubits,” *Phys Rev A* **64**, 052312.
- [60] Kai Wang, Wei Zhang, Zhiyuan Zhou, Mingxing Dong, Shuai Shi, Shilong Liu, Dongsheng Ding, and Baosen Shi, “Optical storage of orbital angular momentum via rydberg electromagnetically induced transparency,” *Chinese Optics Letters* **15**, 060201 (2017).

Supporting information of Experimental demonstration of switching entangled photons based on the Rydberg blockade effect

Yi-Chen Yu,^{1,2} Ming-Xin Dong,^{1,2} Ying-Hao Ye,^{1,2} Guang-Can Guo,^{1,2} Dong-Sheng Ding,^{1,2,*} and Bao-Sen Shi^{1,2,†}

¹Key Laboratory of Quantum Information, University of Science and Technology of China, Hefei, Anhui 230026, China.

²Synergetic Innovation Center of Quantum Information and Quantum Physics, University of Science and Technology of China, Hefei, Anhui 230026, China.

(Dated: November 3, 2020)

Experimental time sequence. The repetition rate of our experiment is 200 Hz, and the MOT trapping time is 4.71 ms. The experimental time window is 25 μ s. The magnetic field is switched off during the switch process. The fields of pumps 1 and 2 are controlled by two AOMs, and therefore the frequencies of signals 1 and 2 photons can be tuned. The optical depth in MOT 1 is about 20. Each of the two lenses with a focal length of 300 mm, is used to couple the signal fields into the atomic ensemble in MOT 1. The short-focus lens (the blue lens in figure 1) with a focal length of 30 mm is used to couple the signal-2 field into the atomic ensemble in MOT 2. The fields of P1 and P2 are collinear, and the signal fields S1 and S2 are collinear. The phase matching condition $k_{p1} - k_{s1} = k_{p2} - k_{s2}$ is satisfied in the spontaneous four-wave mixing process. The two signal photons are collected into their respective single-mode fibers and are detected by two single-photon detectors (avalanche diode, PerkinElmer SPCM-AQR-16-FC, 60% efficiency, maximum dark count rate of 25/s). The two detectors are gated by an arbitrary function generator. The gated signals from the two detectors are then sent to a time-correlated single-photon counting system (TimeHarp 260) to measure their time-correlated function.

Generating entangled photons. We generate entangled photon pairs in MOT 1 which is presented in the upper half of fig.1 (c). We generate the entangled photons via SFWM process by using the counter-propagating pump fields 1 and 2. The SFWM process is based on double- Λ atomic configuration with energy levels of ground state $|1\rangle$, metastable state $|3\rangle$, excited states $|2\rangle$ and $|4\rangle$, which correspond to $5S_{1/2}(F=2)$, $5S_{1/2}(F=3)$, $5P_{1/2}(F=3)$ and $5P_{3/2}(F=3)$. Pump 1 at 795 nm with horizontal polarization is from an external-cavity diode laser (DL100, Toptica). Pump 2 at 780 nm with vertical polarization into the atomic medium is from another external-cavity diode laser (DL100, Toptica). These two pump lasers with different polarizations are propagating in a strictly collinear geometry, with an angle of 2° away from the direction of collected photons [1]. Signal 1 and signal 2 photons are non-classically correlated [2]. Afterwards, we form a phase self-stabilized multiplexing structure where the relative phase between different signal paths can be eliminated because of the symmetrical structure, by using the beam displacer 1, beam displacer 2 and two half-wave plates. Then, signal 1 and signal

2 photons are not only non-classical correlated but also polarization entangled. The form of the entanglement is $|\psi\rangle = (|H_{s1}\rangle|V_{s2}\rangle + e^{i\theta}|V_{s1}\rangle|H_{s2}\rangle)/\sqrt{2}$. In Ref [3], we have already checked the self-stabilization of our structure and the high fidelity of polarization entanglement. We can produce all four Bell states by adjusting the two BDs.

Theoretical analysis. We use the Lindblad master equation: $d\rho/dt = -i[H, \rho]/\hbar + L/\hbar$ in the absence of Rydberg-mediated interactions to characterize the interaction of the EIT light fields with an ensemble of three level atoms, where ρ is the the atomic ensemble's density matrix and H is the atom-light interaction Hamiltonian summed over all the single-atom Hamiltonians under rotating wave approximation with $H = \sum_k H[\rho^{(k)}]$.

$$H[\rho^{(k)}] = -\frac{1}{2}\hbar \begin{pmatrix} 0 & \Omega_p & 0 \\ \Omega_p & -2\Delta_p & \Omega_c \\ 0 & \Omega_c & -2(\Delta_p + \Delta_c) \end{pmatrix}$$

The Lindblad superoperator $L = \sum_k L[\rho^{(k)}]$ is comprised of the single-atom superoperators. The Lindblad master equation includes both spontaneous emissions and dephasing. Ω_p and Ω_c are the Rabi frequency of the probe and coupling light. Δ_p and Δ_c are the detuning of probe and coupling light, respectively. Considering the dephasing of Rydberg state, we introduce γ_d to characterize the decoherence. Since the dephasing of Rydberg state doesn't include population transfer, it ought to be included only as a decay of the coherence, that is in the off-diagonal terms of the Lindblad operator. The single-atom Lindblad superoperator is :

$$2L[\rho^{(k)}]/\hbar =$$

$$\begin{pmatrix} 2\Gamma_e \rho_{ee}^{(k)} & -\Gamma_e \rho_{ge}^{(k)} & -\Gamma_r \rho_{gr}^{(k)} \\ -\Gamma_e \rho_{eg}^{(k)} & -2\Gamma_e \rho_{ee}^{(k)} + 2\Gamma_r \rho_{rr}^{(k)} & -(\Gamma_e + \Gamma_r) \rho_{er}^{(k)} \\ -\Gamma_r \rho_{rg}^{(k)} & -(\Gamma_e + \Gamma_r) \rho_{re}^{(k)} & -2\Gamma_r \rho_{rr}^{(k)} \end{pmatrix}$$

+

$$\begin{pmatrix} 0 & -\gamma_{de} \rho_{ge}^{(k)} & 0 \\ -\gamma_{de} \rho_{eg}^{(k)} & 0 & -\gamma_{de} \rho_{er}^{(k)} \\ 0 & -\gamma_{de} \rho_{re}^{(k)} & 0 \end{pmatrix}$$

+

$$\begin{pmatrix} 0 & 0 & -\gamma_{dr}\rho_{gr}^{(k)} \\ 0 & 0 & -\gamma_{dr}\rho_{er}^{(k)} \\ -\gamma_{dr}\rho_{rg}^{(k)} & -\gamma_{dr}\rho_{re}^{(k)} & 0 \end{pmatrix}$$

where Γ_e and Γ_r are the natural population decay rates of excited state $|e\rangle$ and Rydberg state $|r\rangle$, respectively. γ_{de} and γ_{dr} are the decay of the coherence of excited state $|e\rangle$ and Rydberg state $|r\rangle$ caused by collisions and stray fields. We solve the Lindblad master equation under the condition of steady state corresponding to $t \rightarrow \infty, d\rho/dt = 0$ to get ρ_{eg} . The complex susceptibility of the EIT medium is $\chi = (N|\mu_{ge}|^2/\epsilon_0\hbar)\rho_{eg}$ [4], with N being the atom number density in the medium, and μ_{ge} being the electric dipole moment of the state $|g\rangle \rightarrow |e\rangle$. Under the plane-wave approximation, the transmission of the signal-2 photon through the EIT medium can be obtained from the susceptibility via $e^{-2\text{Im}[w_{s2}/c(1+\chi/2)]L}$, where L is the length of the atomic medium, w_{s2} the frequency of the signal-2 photon, c the speed of light in a vacuum. We calculate the complex linear susceptibility [5]:

$$\chi = \frac{\alpha_0}{k_0} \frac{\Omega_c^2 - 4(\Delta w_{s2} + \delta\Delta + i\gamma_{rg})\gamma_{eg}}{\Omega_c^2 - 4(\Delta w_{s2} + \delta\Delta + i\gamma_{rg})(\Delta w_{s2} + \delta\Delta + i\gamma_{eg})} \quad (1)$$

where $\alpha_0 = OD/L$ is the absorption coefficient when the coupling field is not present, OD is the optical depth of atomic ensemble. k_0 is the wave vector. Δw_{s2} is the detuning of the signal-2 photon. $\delta\Delta$ is the frequency shift used for fitting EIT spectrum. $\gamma_{eg} = \Gamma_e + \gamma_{de}$ is the decay rate of atomic transition $|e\rangle \rightarrow |g\rangle$ corresponding to the natural linewidths of $|e\rangle$. $\gamma_{rg} = \Gamma_r + \gamma_{dr}$ is the decay rate of atomic transition $|nD\rangle \rightarrow |g\rangle$ [6]. Ω_c represents the Rabi frequency of the coupling field. We use this equation 1 to simulate the results given in figure 1 (a) and (b). The strong dipole interaction couples the nearby Rydberg atoms so that the evolution of these atoms are fundamentally linked, thereby modifying the individual atomic energy levels [7]. As a result of the Rydberg dipole interactions, the behaviour of an ensemble of N -atoms cannot simply be described by summing the response of a single atom N times. To describe the behavior for Rydberg-EIT with a gate field, we introduce γ_d to characterize the decoherence to fit the data from our experimental result. If there are no Rydberg dipole interactions, the transmission of the N -atom system can be traced to a summation of N single-atom contributions. γ_d would increase when the Rydberg atoms interact, and the response of each atom is modified significantly. Because of this process, the response of Rydberg atoms would exhibit non-transparency behavior for signal photons when γ_{dr} is large enough. Thus, we can control the single-photon transmission behavior of Rydberg-EIT depending on whether nearby Rydberg atoms are excited.

In our experiment, the coupling Rabi frequency is higher than the polarization decay rate of the excited state but not much higher enough to absolutely separate the two absorption spectra [8]. Furthermore, we have checked the linear susceptibility under the condition of either EIT or AT effect, confirming that the result can be used in all value of Ω_c . Our scheme of switching an entangled photon could work well under both EIT and AT conditions.

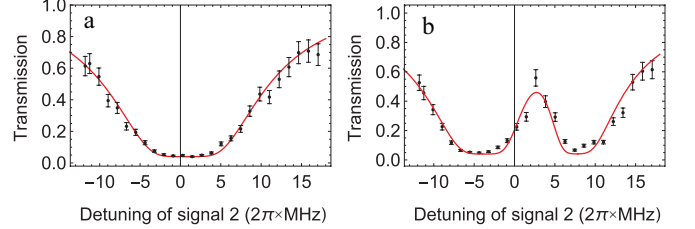


Figure 1. Transmission of the signal-2 photon under different conditions. (a) Absorption spectra of the signal-2 photon with atoms present in MOT 2. The data are fitted by function $e^{-2\text{Im}[w_{s2}/c(1+\chi/2)]L} + a_0$ (solid lines) with parameter values of $\Omega_c = 0$, $\gamma_{eg} = 2\pi \times 3$ MHz, $\gamma_{rg} = 2\pi \times 1$ MHz, $OD = 20$, and $a_0 = 0.04$. (b) Rydberg-EIT effect of the signal-2 photon with coupling field present. The data are fitted by the same function above with parameter values of $\Omega_c = 2\pi \times 11$ MHz, $\gamma_{eg} = 2\pi \times 3$ MHz, $\gamma_{rg} = 2\pi \times 0.1$ MHz, $OD = 20$, $a_0 = 0.04$ and detuning shift $\delta\Delta = -2\pi \times 3.2$ MHz.

Frequency matching between signal 2 and atoms in MOT 2. We need to match the frequency windows to connect two different physical systems. For this point, the emitted signal-2 photon from MOT 1 may not be matched with the working window of Rydberg-EIT in MOT 2. The detuning of the signal-2 photon is performed by changing the frequency of the pump-2 field, which is controlled by an AOM. The pump 2 field passes through the AOM with a frequency shift from $-2\pi \times 12 \sim 2\pi \times 17$ MHz. There is another AOM added in the optical path to give the signal-2 photon (see figure 1 (c) in main text) a frequency shift with $+2\pi \times 120$ MHz. By this method, the frequency of the signal-2 photon can be tuned from the atomic transition $5S_{1/2}(F = 3) \rightarrow 5P_{3/2}(F' = 3)$ to the atomic transition $5S_{1/2}(F = 3) \rightarrow 5P_{3/2}(F' = 4)$. To check whether the signal-2 photon falls into the atomic transition window $5S_{1/2}(F = 3) \rightarrow 5P_{3/2}(F' = 4)$ in MOT 2, we measure its absorption and EIT transmission spectra (figure 3) by changing the frequency of the emitted signal-2 photon. To check this process, we added a coupling field, which is resonant with the atomic transition $5P_{3/2}(F' = 3) \rightarrow 5D_{5/2}$ to demonstrate the Rydberg-EIT.

Time dependence of the transmission spectrum of Rydberg- D state. The Ref. [9] has reported the dephasing of Rydberg- D state polaritons, namely, time dependence of the transmission on EIT resonance. As

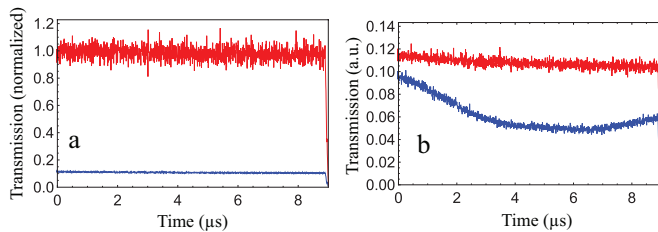


Figure 2. (a) The normalized transmission of probe field on Rydberg-EIT resonance. The red line represents 1.5 photons/ μs , the blue line corresponds to 38.7 photons/ μs . (b) Time dependence of probe transmission with different photons (not normalized, only see the profile of the transmission line). The red line represents 38.7 photons/ μs , the blue line corresponds to 601.4 photons/ μs .

stated in this reference, the Rydberg- D state dephasing effect is caused by the interaction-induced coupling to degenerate Zeeman sublevels, preventing other photons propagating through the cloud. We also checked the D -state dephasing in our experiment to demonstrate probe field transmission under the EIT resonance condition. We use a probe field with 1.5 photons/ μs as an input field, the transmission is higher than using 38.7 photons/ μs , (see the results given in Fig. 2 (a)). We want to show that the gate field with 1.5 photon/ μs is not enough to reach a strong quantum nonlinearity to obviously destroy the transparency. Thereby, the transmission rate is almost 1 (actually lower than 1). But the strong interaction between Rydberg atoms could easily tunes the transition out of resonance on the condition of the gate field with 38.7 photons/ μs . The comparison is consistent with the result of our experiment. And the gate field is almost 15.5 photons/ μs during our experiment. We use the normalized transmission in the left panel to distinguish the transmission rate under two different conditions. The Rydberg- D state dephasing is not obvious for small photon numbers, but with an obvious time dependence with much more photon numbers, given in Fig. 2 (b). So, the D -state dephasing caused by the gate field is not obvious in our experiment, for the gate photon number we used in our experiment is 15.5 photons/ μs , which is smaller than 38.7 photons/ μs . In addition, we also compared the Rydberg-EIT effects for D state and S state by tuning the coupling laser wavelength, the only difference between them in our configuration is the height of the transparent peak with the transparent peak of D state higher than that of S state. In order to obviously observe the blockade effect in Rydberg-EIT, we choose Rydberg- D state to demonstrate the experiment.

Nonlinear response of Rydberg blockaded ensemble. We provide the visualized evidence of nonlinear response of Rydberg blockaded ensemble. Before the switch operation in our experiment, we change the input

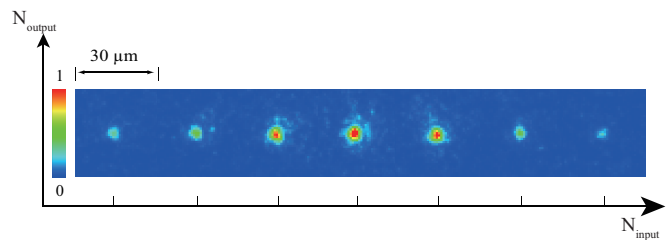


Figure 3. We change the input photon numbers N_{input} from a weak coherent light beam. Then we record the output photon numbers N_{output} after the propagation through the MOT 2 proving that N_{output} nonlinearly increase as N_{input} increase.

photon numbers (N_{input}) of signal-2 photons which are from a weak coherent light beam. Then we record the output photon numbers (N_{output}) after the propagation through the MOT 2 Rydberg-EIT transparent window by a fast and high-efficient camera (PI-MAX 4, princeton instruments) shown in Fig. 3. As we increase N_{input} , N_{output} nonlinearly increase or even decrease because of the Rydberg-blockade effect. Thus, there is a threshold in our Rydberg ensemble. If the input photon numbers exceed that threshold, our ensemble exists large nonlinearity to block the input photons. In fact, the gate field is applied to our ensemble to approach that threshold.

* dds@ustc.edu.cn

† drshi@ustc.edu.cn

- [1] Kaiyu Liao, Hui Yan, Junyu He, Shengwang Du, Zhi-Ming Zhang, and Shi-Liang Zhu, “Subnatural-linewidth polarization-entangled photon pairs with controllable temporal length,” *Phys. Rev. Lett.* **112**, 243602 (2014).
- [2] Dong-Sheng Ding, Zhi-Yuan Zhou, Bao-Sen Shi, Xu-Bo Zou, and Guang-Can Guo, “Generation of non-classical correlated photon pairs via a ladder-type atomic configuration: theory and experiment,” *Optics express* **20**, 11433–11444 (2012).
- [3] Yi-Chen Yu, Dong-Sheng Ding, Ming-Xin Dong, Shuai Shi, Wei Zhang, and Bao-Sen Shi, “Self-stabilized narrow-bandwidth and high-fidelity entangled photons generated from cold atoms,” *Phys. Rev. A* **97**, 043809 (2018).
- [4] Stephen E Harris, JE Field, and A Imamoglu, “Nonlinear optical processes using electromagnetically induced transparency,” *Physical Review Letters* **64**, 1107 (1990).
- [5] Shanchao Zhang, JF Chen, Chang Liu, Shuyu Zhou, MMT Loy, George Ke Lun Wong, and Shengwang Du, “A dark-line two-dimensional magneto-optical trap of 85rb atoms with high optical depth,” *Review of Scientific Instruments* **83**, 073102 (2012).
- [6] U. Raitzsch, R. Heidemann, H. Weimer, V. Bendkowsky, and T. Pfau, “Investigation of dephasing rates in an interacting rydberg gas,” *New Journal of Physics* **11**, 6456–6460 (2008).
- [7] James Keaveney, *Collective Atom-Light Interactions in Dense Atomic Vapours* (Springer, 2014).
- [8] Tony Y. Abi-Salloum, “Interference between competing

- pathways in the interaction of three-level ladder atoms and radiation,” *Journal of Modern Optics* **57** (2007), [10.1080/09500341003658147](https://doi.org/10.1080/09500341003658147).
- [9] Christoph Tresp, Przemyslaw Bienias, Sebastian Weber, Hannes Gorniaczyk, Ivan Mirgorodskiy, Hans Peter Büchler, and Sebastian Hofferberth, “Dipolar dephasing of rydberg d-state polaritons,” *Phys. Rev. Lett.* **115**, [083602](https://doi.org/10.1103/PhysRevLett.115.083602) (2015).